Published in final edited form as:
Nat Cell Biol. 2009 March ; 11(3): 286–294. doi:10.1038/ncb1836.

Electrochemical cues regulate assembly of the Frizzled/Dishevelled complex at the plasma membrane during planar epithelial polarization

Matias Simons[1], **William J. Gault**[1], **Daniel Gotthardt**[2], **Rajeev Rohatgi**[3], **Thomas J. Klein**[1], **Youming Shao**[4], **Ho-Jin Lee**[4], **Ai-Luen Wu**[5], **Yimin Fang**[5], **Lisa M. Satlin**[3], **Julian T. Dow**[6], **Jie Chen**[5], **Jie Zheng**[4], **Michael Boutros**[7], and **Marek Mlodzik**[1]

[1]Department of Developmental and Regenerative Biology, Mount Sinai School of Medicine, One Gustave L. Levy Place, New York, NY 10029, USA.

[2]Department of Medicine, Division of Gastroenterology, University Hospital Heidelberg, D-69120 Heidelberg, Germany.

[3]Department of Pediatrics, Mount Sinai School of Medicine, One Gustave L. Levy Place, NY, NY 10029, USA.

[4]Department of Structural Biology, St. Jude Children's Research Hospital, Memphis, TN 38105, USA.

[5]Department of Cell and Developmental Biology, University of Illinois at Urbana-Champaign, 601 South Goodwin Avenue, Urbana, IL 61801, USA.

[6]Institute of Biomedical and Life Sciences, Division of Molecular Genetics, University of Glasgow, Glasgow, UK.

[7]German Cancer Research Center, Division of Signaling and Functional Genomics, Im Neuenheimer Feld 580, D-69120 Heidelberg, Germany.

Abstract

Dishevelled (Dsh) is a cytoplasmic multidomain protein that is required for all known branches of the Wnt signalling pathway1−3. The Frizzled/planar cell polarity (Fz/PCP) signalling branch requires an asymmetric cortical localization of Dsh, but this process remains poorly understood. Using a genome-wide RNA interference (RNAi) screen in *Drosophila melanogaster* cells, we show that Dsh membrane localization is dependent on the Na^+/H^+ exchange activity of the plasma membrane exchanger Nhe2. Manipulating Nhe2 expression levels in the eye causes PCP defects, and Nhe2 interacts genetically with Fz. Our data show that the binding and surface recruitment of Dsh by Fz

1,8Correspondence should be addressed to M.M. (marek.mlodzik@mssm.edu).

Note: Supplementary Information is available on the Nature Cell Biology website.

AUTHOR CONTRIBUTIONS

M.S. coordinated the project, designed and conducted the RNAi screen, performed the experimental work and data analysis and wrote the manuscript. W.J.G. performed the pupal dissections. W.J.G. and D.G. assisted with experiments. T.J.K. helped with the RNAi screen assay. R.R. and L.S.M. performed pH measurements. Y.S., H.-J.L. and J.Z. purified the DEP domain and performed electrostatic potential calculations. A.-L.W., Y.F. and J.C. performed SUV lipid binding assays. J.T.D. provided Nhe2 tools. M.B. designed and conducted the RNAi screen. M.M. coordinated the project, assisted with planning the experiments and data analysis and wrote the manuscript.

COMPETING FINANCIAL INTERESTS

The authors declare no competing financial interests.

is pH- and charge-dependent. We identify a polybasic stretch within the Dsh DEP domain that binds to negatively charged phospholipids and appears to be mechanistically important. Dsh recruitment by Fz can be abolished by converting these basic amino-acid residues into acidic ones, as in the mutant, DshKR/E. *In vivo*, the DshKR/E(2×) mutant with two substituted residues fails to associate with the membrane during active PCP signalling but rescues canonical Wnt signalling defects in a *dsh*-background. These results suggest that direct interaction between Fz and Dsh is stabilized by a pH and charge-dependent interaction of the DEP domain with phospholipids. This stabilization is particularly important for the PCP signalling branch and, thus, promotes specific pathway selection in Wnt signalling.

Membrane recruitment of Dsh is an important aspect of both canonical (β-Catenin) and non-canonical (PCP) Wnt signalling[1,4]. In canonical signalling, Wnt ligands trigger the formation of Dsh-dependent signalosomes at the plasma membrane5. Similarly, asymmetric membrane association of Dsh is a key event in the Wnt-Fz/PCP signalling branch (for reviews see refs 2 and 3). It remains unclear whether the membrane association of Dsh in canonical and PCP signalling uses the same mechanism.

Dsh consists of three domains, DIX, PDZ and DEP, and binds weakly to Fz via its PDZ domain through a conserved KTxxxW motif in the Fz carboxyl terminus[6]. The DEP domain is also important in membrane targeting as it is both necessary and sufficient for Fz-dependent recruitment[7]. However, no binding site for Fz has yet been identified in the DEP domain. Based on the structure of the DEP domain, it has been suggested that a polybasic amino acid stretch could interact with acidic and negatively charged lipids in the membrane[8].

To newly identify components required for the stable formation of Fz–Dsh complexes at the plasma membrane, we developed a cell-based assay that is applicable for high-throughput approaches (Fig. 1a–e). In *D. melanogaster* S2R+ cells (as well as in other cell lines) co-expression of Fz with Dsh–GFP led to efficient recruitment of Dsh–GFP to the membrane[9] (Fig. 1b, g). Using this assay, we performed a genome-wide RNAi screen for factors required in Fz-mediated Dsh–GFP membrane recruitment. Cells were plated into 57 384-well plates, with each well containing long double-stranded RNA against approximately 90% of all *D. melanogaster* genes[10], and were then transfected with Dsh–GFP and Myc-Fz plasmids (Fig. 1a, b). The plates were analysed and scored by visual inspection using a fluorescence microscope (see Methods). Apart from the positive controls (*fz, dsh, par-1*11), the screen identified several unknown genes and factors known for their role in protein trafficking (for example SNAP). These latter factors were shown to block Fz-transport thereby inhibiting Dsh membrane recruitment (data not shown).

One candidate with an annotated function was *Nhe2* (CG9256). The protein Nhe2 belongs to a family of sodium/proton exchangers (NHEs). Cellular pH homeostasis is regulated by NHEs through the extrusion of protons in exchange for sodium ions in most organellar membranes, including the plasma membrane[12,13]. In *D. melanogaster*, there are three NHEs, that have not yet been characterized functionally. When compared with human NHEs, *D. melanogaster Nhe2* has the highest sequence homology to human *NHE3*, which encodes for a plasma membrane exchanger. These type of NHEs have been implicated in the formation of alkaline pH and charge microenvironments at the plasma membrane[14]. In polarized cell migration, localized NHEs activity leads to the activation of Rho family GTPases and actin polymerization[15]. As these are important downstream events in PCP signalling, we decided to analyze the role of Nhe2 in Dsh recruitment more closely.

First, to confirm the data from *D. melanogaster* S2R+ cells, we silenced human *NHE3* with short interfering RNA (siRNA) in HEK293T cells, which also impaired Fz-mediated Dsh recruitment (Fig. 1g, h; Supplementary Information, Fig. S1a, b). This suggests that the role

of Nhe2 in Dsh recruitment is conserved, and also rules out potential off-target effects associated with the *Nhe2* dsRNA. Consistent with other reports[16] the *NHE3* knockdown did not seem to affect the global pH within the cell (Supplementary Information, Fig. S1e). However, we were able to partially rescue the recruitment defect seen in the *NHE3* knockdown cells by transient alkalinization (Fig. 1f–i). In a similar manner, treatment of HEK293T cells expressing Fz and Dsh with the selective NHE3 inhibitor S3226, but not the NHE1 inhibitor cariporide, effectively redistributed Dsh into the cytoplasm (Fig. 1d, e; data not shown; Supplementary Information, Fig. S2c). From these results, we can conclude that it is the proton-translocation function of NHE3 that is required for Dsh localization. To phenocopy the absence of sodium/proton exchange at the membrane we reduced the intracellular pH (pH_i) in S2R+ cells using two independent methods (Fig. 1j–p). Both treatments led to defects in Dsh recruitment; however they did not affect Fz transport to the surface (Fig. 1k–m). In contrast, reduced pH_i did not inhibit the membrane recruitment of Pk, another PCP core protein, to cell–cell contact sites (Supplementary Information, Fig. S2a, b). Nor did reducing pH_i affect the membrane association of the lactadherin C2 domain (LactC2), which binds to phosphatidylserine in a charge-independent manner (Fig. 1n–p). This is in accordance with the finding that the inhibitor S3226 also had no effect on LactC2 membrane association[17] (Supplementary Information, Fig. S2c).

In the *D. melanogaster* eye, PCP is generated in ommatidial preclusters when Fz/PCP signalling specifies the cell fates of photoreceptors R3 and R4 (thus defining the chiral form of each ommatidium seen in adult eyes), which is followed by a 90° rotation of each ommatidial cluster towards the dorso-ventral midline[2] (the equator). This results in a mirror-image ommatidial arrangement across the equator (Fig. 2a). One of the key events in Fz/PCP signalling is asymmetric Dsh membrane association[2,3]. We therefore tested whether Nhe2 has a role in Fz/PCP signalling in the *D. melanogaster* eye, where PCP defects manifest as chirality inversions, symmetrical cluster formations and rotation defects of ommatidia[2]. *Nhe2* has two splice variants that differ in the length of their C termini[18] (Supplementary Information, Fig. S3). Overexpression of both the short and the long form resulted in PCP defects in the eye (Fig. 2b; data not shown). These defects were already detected during development in eye imaginal discs (Supplementary Information, Fig. S4h–j). Consistently, overexpression of NHE3 also impaired Dsh recruitment in HEK293T cells (Supplementary Information, Fig. S1d).

To further test for *Nhe2* requirement in PCP, we generated a loss-of-function mutant allele by imprecise P-element excision. The excision event produced a homozygous-lethal deletion of 6.1 kb (Supplementary Information, Fig. S3). This deletion mutant, $Nhe2^{1}$, is a strong loss-of-function allele with no detectable *Nhe2* transcript by *in situ* hybridization (Supplementary Information, Fig. S3). $Nhe2^{1}$ is homozygous lethal and, importantly, lethality can be rescued by uniform expression of the splice variant *UAS-Nhe2long* (under control of *tub>GAL4*; data not shown), confirming the specificity of the mutant allele. $Nhe2^{1}$ homozygous animals die during early larval stages with defects in gut morphology and function, and fat body development (Supplementary Information, Fig. S3, legend). Clonal analyses showed that homozygous $Nhe2^{1}$ clones cannot be recovered in adult or larval tissue (data not shown), precluding PCP analysis and indicating that *Nhe2* is required for cell viability. However, expression of *Nhe2* RNAi ($Nhe2^{IR}$) in a heterozygous $Nhe2^{1}$ condition using an eye-specific driver caused PCP defects in the eye (Fig. 2c). This genetic combination also showed phenotypes related to general eye morphology and thus it was difficult to further enhance the PCP defects and still maintain scorable tissue. Similarly, in other tissues, such as the wing, $Nhe2^{IR}$ had pleiotropic effects and did not allow scoring of PCP defects (data not shown).

Based on the gain- and loss-of-function eye PCP phenotypes, we tested *Nhe2* for genetic interactions with core PCP genes. Removing one copy of *Nhe2* in combination with $Nhe2^{IR}$ suppressed the dominant Fz overexpression eye phenotype (*sev>Fz*; Fig. 2d–f)[9]. In addition,

co-expression of Nhe2 and Fz enhanced the phenotype when compared with Fz alone (Supplementary Information, Fig. S4a–c). No genetic interactions of *Nhe2* were detected with the PCP-phenotypes Fmi or Stbm (Supplementary Information, Fig. S4d–f, data not shown), suggesting that *Nhe2* interacts specifically with *fz*. Apart from the genetic interactions, Nhe2 and Fz also interacted physically, as detected in co-immunoprecipitates from HEK293T cells (Supplementary Information, Fig. S1c). We did not detect a genetic interaction with *sev>Dsh*, similar to a lack of dominant interaction between *fz* and *sev>Dsh*. This is consistent with Nhe2 functioning, like Fz, upstream of Dsh. These results suggest that Nhe2 modulates Fz function *in vivo* and may do so by regulating a pH-dependent Dsh recruitment.

Molecular interactions dependent on pH often involve charged binding sites. The Dsh DEP domain contains a positively charged amino-acid cluster that may interact with negatively charged surfaces, such as acidic lipid headgroups, in the membrane (Fig. 3a). To test this hypothesis, we conducted lipid-binding assays using small unilamellar vesicles (SUVs) with various phospholipids. SUVs were made with 50% phosphatidylcholine (PC) to ensure stability. The DEP domain preferentially bound to phosphatidic acid (PA) and phosphatidylglycerol (PG), which have a negative charge at physiological pH, but not to PC and phosphatidylethanolamine (PE) which form neutral zwitterions (Fig. 3b). This suggests that the DEP domain interacts with lipids in an electrostatic manner. To determine the extent to which inner surface potential can contribute to the binding, we modelled the interaction, using the non-linear Poisson-Boltzmann equation to calculate electrostatic potentials. Charge calculations were performed on wild-type DEP (DEPwt) and a DEP mutant in which the polybasic amino acid stretch was converted into a polyacidic stretch (DEPK/E). The binding energy (ΔG) of DEPwt and the acidic lipid membrane (PC/PA at 1:1 ratio) was predicted to be favorable ($\Delta G = -40.7$ kcal mol^{-1}). The data for DEPK/E, however, showed a positive binding energy ($\Delta G = 58.5$ kcal mol^{-1}), which does not allow interaction (Fig. 3c).

To confirm these models experimentally, we tested the ability of DEPwt and DEPK/E to bind phospholipid SUVs. The overall structure of DEPK/E was unchanged relative to DEPwt as determined by chemical shift patterns in NMR spectroscopy (data not shown). As predicted, binding of DEPK/E to PA/PC SUVs was markedly impaired (Fig. 3d). In an independent assay, we confirmed that DEPwt specifically interacted with PA, which was spotted among an array of phospholipids, whereas DEPK/E failed to interact with any lipids (Fig. 3e).

Next, we asked whether the same charge-dependent mechanism also has a role in the recruitment of Dsh by Fz in live cells. We introduced the same lysine- or arginine-to-glutamic acid changes in the DEP domain of full-length *D. melanogaster* Dsh–GFP, which did not compromise protein stability (Supplementary Information, Fig. S5b). These mutations in the resulting mutant, DshKR/E, dramatically interfered with Fz-mediated membrane recruitment in S2R+ cells (Fig. 4a–f), HEK293T cells (data not shown), and importantly, also *in vivo* in native wing-disc epithelia (Fig. 4k–l). When up to five basic amino acids were mutated, DshKR/E(5×), Dsh recruitment by Fz was abolished, suggesting that negative charge on the DEP domain surface counteracts membrane recruitment (Fig. 4a–l). To further confirm this hypothesis we tested the effect of charges on the membrane. Strikingly, the application of sphingosine, a cationic lipid that reduces the negative charges of the inner surface, impaired Dsh co-localization with Fz at the membrane (Fig. 4m–r; it did not affect LactC2 membrane localization, Supplementary Information, Fig. S2c)[19,17]. In contrast, sphingosine treatment allowed effective association of the DshKR/E mutant with Fz at the membrane, suggesting that the neutralization of surface charge rescues repulsion of the DshKR/E mutant from the membrane (Fig. 4s–y).

For the most stringent test, we investigated whether the DshKR/E mutations affect Dsh function *in vivo* by using rescue assays of the *dsh*$^{-}$ genotype. We expressed various Dsh mutants,

mutated at the polybasic stretch, under the endogenous *dsh* promoter in a *dsh* null background (*dsh*^{V26}*; dsh>dsh–GFP*). Dsh is required for both the canonical and the non-canonical Wnt pathway, which govern distinct developmental processes. Therefore, the expression of Dsh constructs in this background allowed us to assess the importance of polybasic stretch-mediated membrane recruitment for either Wnt/β-cat signalling or the Fz/PCP pathway. Using this assay, we found that complete conversion of the polybasic stretch, DshKR/E(5×), failed to rescue *dsh*^{V26} lethality and therefore canonical Wnt/β-cat signalling. However, the replacement of only two basic residues with acidic ones (see Methods), generating DshKR/E(2×), produced viable flies with no apparent defects in the canonical Wnt/β-cat pathway. In contrast, these flies showed mild PCP defects in the eye (Fig. 5a–b) and severe PCP defects in the wing (Fig. 5c–d, q–r). As acute overexpression of Fz can still recruit DshKR/E(2×) to the membrane (Supplementary Information, Fig. S5a), membrane localization of this mutant, unlike DshKR/E(5×), is not fully defective, which probably explains the absence of canonical Wnt phenotypes (Fig. 5e–f; data not shown). However, immunostaining of the pupal wing epithelium showed that during critical phases of active PCP signalling, *dsh>dshKR/E(2×)* fails to associate with the cell cortex (Fig. 5g–r). Therefore, we conclude that membrane association of Dsh mediated by the polybasic stretch in the DEP domain is necessary for proper PCP signalling *in vivo*, but seems to be dispensable for canonical Wnt signalling.

Taken together, our data demonstrate that Dsh membrane recruitment during PCP signalling is dependent on electrostatic interactions of the DEP domain with negatively charged phospholipids (such as PA). According to the biophysical properties of these lipids, their negative charge should be maintained by a more alkaline pH[20]. Therefore we speculate that proximity to a Nhe should facilitate the interaction by maintaining a low proton concentration below the membrane. In our model, Dsh binds to the KTxxxW motif of Fz via its PDZ domain, and directly to the membrane via its DEP domain (Fig. 5s). Under lower pH conditions or after neutralization of the membrane surface charge, the positively charged Dsh DEP domain is repelled from the membrane. Similarly, when the DEP domain bears a polyacidic amino acid cluster, Dsh is also repelled from the membrane (Fig. 5s).

Despite the strong Fz/Dsh association at the membrane, the interaction of the Dsh-PDZ domain with Fz has been reported to be weak (K_d~10 μM)[6]. It is therefore likely that other interacting surfaces and modes exist that stabilize the interaction. Although it cannot be excluded that the DEP domain can also bind directly to Fz in a pH- and charge-dependent manner, our studies show that reducing the amount of negatively charged lipids in the plasma membrane (using neutralizing agents such as sphingosine) has strong effects on the localization of wild-type and mutant Dsh (Fig. 4m–y). Dsh may first bind to Fz.This interaction could then be stabilized by the attraction of the Dsh DEP domain to the negatively charged lipids of the plasma membrane, although the opposite is equally possible. In either case, the phospholipid-binding DEP domain would cooperate with the specific (but low-affinity) Fz-binding PDZ domain to recruit Dsh specifically to membranes that are enriched in acidic phospholipids and Fz. Such cooperative binding is used by many proteins to increase the specificity of their membrane association, and allows for integration of complex signalling input[21].

A characteristic feature of Dhs function is that it is able to signal in different Wnt pathways. What determines the signalling specificity remains so far unknown. Most canonical Wnt-signalling mutations in *D. melanogaster* Dsh are not found in the DEP domain[22]. Unlike the DIX domain, the DEP domain has also been shown to be dispensable for LRP6 phosphorylation occurring in signalosomes at the membrane[23]. In contrast, all PCP-specific mutations (including *dsh*^{1}) are located in the DEP domain and impair stable Dsh membrane recruitment. It is therefore possible that specific Wnt pathway activation requires conformational changes in the Dsh protein that lead to differential domain exposure with different effects on membrane recruitment. Here, we describe a mechanism for a DEP-mediated membrane recruitment that

is particularly important for PCP signalling. We propose that distinct membrane lipids can promote a stable Fz/Dsh interaction at the surface, which is pH- and charge-dependent, and regulated by local Na^+/H^+-exchange activity. Future studies will be directed at determining whether local electrochemical cues could serve as general determinants in the spatial control of signalling events that lead to cell and tissue polarization.

METHODS

Cell Culture

S2R+ cells were maintained at 25 °C in Schneider's medium (Invitrogen) and HEK293T cells were maintained at 37 °C in Dulbecco's MEM (GIBCO) in a humidified atmosphere with 5% CO_2. both media were supplemented with 10% fetal calf serum (PAA) and 50 μg ml^{-1} penicillin/streptomycin.

Genetics and phenotypic analysis

Overexpression and transgenic RNAi studies were performed using the GAL4/UAS system (RNAi crosses grown at 29 °C, other crosses at 25 °C; w^{1118} was control). *Nhe2*^{1} was generated by P-element excision of EY11323 and mapped by PCR. *UAS-fz, UAS-dsh, UAS-stbm* and *UAS-fmi* strains were as described previously[1,24]. *sev-GAL4* was an eye-specific driver and *dpp>GAL4* was for expressing Myc–Fz at the A/P boundary in the wing. Flip-out clones were generated with *hsflp; act5C>CD8>GAL4; mδlacZ*. For *dsh*^{V26} rescue: male flies transformed with *pCaSpeR dsh>dsh*^{wt4} or the respective *dshKR/E* isoforms were crossed with *y,w,dsh*^{V26} *f*^{36A}/FM6 females. For assessment of rescue, male *y,w* larvae or male *f*^{36A} non-FM6 flies were selected and processed for pupal wing immunohistochemistry, and adult eye and wing analysis. For each genotype, 3–6 independent eyes were scored. Third- instar eye and wing discs were processed for immunohistochemistry as described previously[24]. Antibodies: rat anti-Elav (DSHB) and rabbit anti-βgal (Cappel) for eye discs and mouse anti-Myc 9E10 (Santa Cruz) and rabbit anti-GFP (Molecular Probes) for wing discs . Pupal wings were also stained with TRITC-labelled phalloidin.

Molecular cloning

D. melanogaster Nhe2 has two transcripts with differing lengths of C termini. *Nhe2*short was amplified from EST AT11019 by PCR. For *Nhe2*long, the C-terminal coding region was amplified from cDNAs and fused to the partial EST clone RE21674. Complete *Nhe2*long and short coding sequences were cloned into the UAS-based Gateway vector pTWV (DGRC). For *in-vivo* RNAi hairpin expression, two identical 455 bp *Nhe2* sequences (Probe ID: HFA03172 at http://rnai.dkfz.de/) were cloned in opposite orientations into UAS-based pWIZ vector.

For cell culture experiments, Dsh–GFP and Myc–Fz were subcloned into pAc5.1/V5-His, pMT/V5-His (Invitrogen) or pCS2+ vectors. E^2–GFP (used for pH calibration) was amplified from pcDNA3.1 E^2–GFP (a gift from R. Bizzarri, Scuola Normale Superiore, Pisa)[25] and cloned into pAc5.1 with Dsh–GFP replacing GFP. DshKR/E mutations in pAc5.1 Dsh–GFP were made by Quickchange-PCR (Stratagene). They included R422E, R425E, R426E, R433E, K443E for DshKR/E(5×) and R426E and R433E for DshKR/E(2×). K/E mutations in mouse Dvl1 DEP were made in the pQE vector (Qiagen), including K408E, K458E, K465E, K472E and K482E. Primer sequences available on request.

RNAi experiments

For RNAi experiments in *D. melanogaster* S2R+ cells, dsRNAs were generated from DNA templates by *in vitro* transcription as described previously[10] (sequence information available at http://rnai.dkfz.de/). RNAi screening was performed as reported[10]. Each screen plate

included one negative control (Relish dsRNA) and three positive controls (*fz, par-1* and *dsh*). Relish knockdown did not affect Dsh recruitment, *fz* knockdown resulted in no Dsh recruitment (Dsh–GFP being localized to cytoplasmic aggregates26), *par-1* knockdown in severely impaired recruitment, and *dsh* knockdown in no detectable Dsh–GFP. Control genes were also identified with their respective phenotypes among the RNAi library. Primary screen hits were re-screened three times in a blinded fashion.

For RNAi in HEK293T cells, the cells were transfected with a total of 100 nM siRNA (in the case of NHE3 4 × 25 nM SMARTPool siRNA) using Oligofectamine (Invitrogen). After 24 h, cells were transfected with plasmids encoding *Xdsh*–GFP and HA–Fz4 (a gift from T. Kirchhausen, Harvard Medical School, Boston) or pCS2+ *Dm*Dsh–GFP and pCS2+ Myc–*Dm*Fz respectively (*Dm* represents *D. melanogaster*). *NHE3* knockdown was confirmed by western blotting after mannitol lysis using a rabbit anti-NHE3 (Chemicon)[27]. The protein band pattern was compared with the pattern of transfected rabbit NHE3–HA (provided by J. Orlowski, McGill University, Montreal).

Intracellular acidification/alkanilization and pH measurements

For intracellular acidification, cells were transfected with pMT Dsh–GFP and pAc5.1 Myc–Fz. Six hours after induction of Dsh–GFP expression with $CuSO_4$ (500 mM), cells were prepulsed with NH_4Cl (30 mM) for 30 min and kept for 12–16 h in KCl or NaCl (0.14 M), Hepes (20 mM), $CaCl_2$ (2 mM) and $MgCl_2$ (1 mM) at pH 7.0 (ref. 28). For analysis, cells were stained with anti–Myc 9E10 antibody (Santa Cruz) after fixing with 4% paraformaldehyde and permeabilizing with 0.1% Triton-X100. Complete, partial or no recruitment was scored in cells by measuring Myc–Fz expression at the cell surface. To determine the effects of these treatments on pH_i, S2R+ cells were transfected with pAc5.1 E^2–GFP and imaged with Leica SP3 confocal microscope. Emission ratios were obtained using an excitation wavelength of 476 nm and two emission wavelength intervals of 480–515 nm and 515–600 nm as described[25]. The pH_i was clamped for calibration with high K^+/nigericin (Biomol) at pH 6.8, 7.6 and 8.2 after determining emission ratios at normal conditions. Ratio images were made with ImageJ software. Longer treatments with the same calibration solutions were used as a second method to lower pH_i. For this, pH 6.8 calibration solutions, with or without nigericin, were applied to S2R+ cells (transfected with pAc5.1 Dsh–GFP and pAc5.1 Myc–Fz) for 4 h and processed for immunocytochemistry.

For intracellular alkanilization, HEK293T cells treated with control and *Nhe3* siRNA and transfected with Dsh–GFP and Myc–Fz were kept for 90 min in isotonic solution (140mEq NaCl and 5mEq KCl) with or without 30 mM NH_4Cl. Ratiometric dye BCPCF (Molecular Probes) was used to monitor pH_i, which was subsequently clamped for calibration using the high K^+/nigericin method at pH 6.8 and 7.8. A pH_i rise to more than pH 8.0 was shown, before gradual normalization.

Sphingosine and Nhe inhibitor treatments

Synthetic Sphingosine (Avanti-Polar-Lipids) was applied for 6–12 h (75 μM) to Dsh/Fz-transfected HEK293T or S2R+ cells before fixing and immunostaining with anti-Myc antibody. For rescue of DshKR/E membrane recruitment sphingosine was applied for 3 h.

The Nhe inhibitors S3226 (more specific for NHE3) and cariporide (more specific for Nhe1) were provided by J. Puenter (Sanofi-Aventis). S3226 affected Dsh recruitment in HEK293T cells at > 30 μM. In depicted experiments, S3226 and cariporide were applied for 12 h at 50–100 μM.

All statistical analyses were performed using two-tailed Student's *t*-tests to calculate *P* values (Microsoft Excel).

Protein expression, small unilamellar vesicles (SUV) lipid-binding assays and computational methodology for electrostatic potential calculations

Purification of the mouse Dvl1(Dsh homologue) DEP domain was performed as described previously[8]. The HSQC spectra of mutant DEP domains were obtained to determine whether site-directed mutagenesis affected the structure. The NMR samples consisted of 0.3 mM of the DEP domain (0.3 mM) in phosphate buffer (0.1 M, pH 6.8), EDTA (0.5 mM) and 1,4-dithiothreitol (DTT, 3 mM). We observed that both mutant DEP domains showed a similar chemical shift pattern to wild-type DEP, indicating that the structure of mutant DEP domains was not affected.

Generation of SUV liposomes was as described previously[29]. We generated SUVs with various phospholipids. Vesicles containing PA, PG, PC, and PE were made with 50% PC to ensure stability. For lipid binding assays, vesicles (~5 mM phospholipids) were mixed with purified wild-type or mutant DEP domains in column buffer (40 mM Tris-Cl, pH 7.5, 150 mM NaCl, 2 mM EDTA, 2 mM EGTA and 1 mM DTT), incubated at room temperature for 30 min, and separated by chromatography on a Sephacryl S-300 column. Fractions were analyzed in 13% SDS gels by silver-staining.

To determine whether PA-binding to DEP was specific, PIP (phospho-inosidephosphate) strips (Echelon) were overlayed with purified His-tagged DEPwt and K/E domains in 3%BSA/PBS-0.1% Triton-X100 for 3 h at room temperature. After washing steps with 3%BSA/PBS-0.1% Triton-X100, strips were subjected to standard western blotting with an anti-His antibody (Qiagen).

For computational methodology for electrostatic potential calculations see Supplementary Information.

Supplementary Material

Refer to Web version on PubMed Central for supplementary material.

Acknowledgments

We thank Bloomington Stock Center for fly strains, S. Grinstein, J. Orlowski, T. Kirchhausen and R. Bizzarri for cDNA constructs. We are grateful to A. Jenny and Y. Wang for the cloning of cDNA constructs, and U. Weber for analysis of the embryonic/early larval lethal phenotype. We thank C. Iomini, R. Krauss, S. Sokol and D. del Alamo for reading the manuscript, members of the Mlodzik laboratory for discussions and S. Okello, G. Garcia and M. Stricker for technical support. The work has been supported by NIH grant to M.M. RO1 GM62917. M.S. was a recipient of EMBO and DFG long-term fellowships.

References

1. Boutros M, Paricio N, Strutt DI, Mlodzik M. Dishevelled activates JNK and discriminates between JNK pathways in planar polarity and wingless signaling. Cell 1998;94:109–118. [PubMed: 9674432]
2. Seifert JR, Mlodzik M. Frizzled/PCP signalling: a conserved mechanism regulating cell polarity and directed motility. Nature Rev. Genet 2007;8:126–138. [PubMed: 17230199]
3. Veeman MT, Axelrod JD, Moon RT. A second canon. Functions and mechanisms of β-catenin-independent Wnt signaling. Dev. Cell 2003;5:367–377. [PubMed: 12967557]
4. Axelrod JD. Unipolar membrane association of Dishevelled mediates Frizzled planar cell polarity signaling. Genes Dev 2001;15:1182–1187. [PubMed: 11358862]

5. Bilic J, et al. Wnt induces LRP6 signalosomes and promotes dishevelled-dependent LRP6 phosphorylation. Science 2007;316:1619–1622. [PubMed: 17569865]
6. Wong H-C, et al. Direct binding of the PDZ domain of Dishevelled to a conserved internal sequence in the C-terminal region of Frizzled. Mol. Cell 2003;12:1251–1260. [PubMed: 14636582]
7. Rothbacher U, et al. Dishevelled phosphorylation, subcellular localization and multimerization regulate its role in early embryogenesis. EMBO J 2000;19:1010–1022. [PubMed: 10698942]
8. Wong HC, et al. Structural basis of the recognition of the dishevelled DEP domain in the Wnt signaling pathway. Nature Struct. Biol 2000;7:1178–1184. [PubMed: 11101902]
9. Boutros M, Mihaly J, Bouwmeester T, Mlodzik M. Signaling specificity by Frizzled receptors in *Drosophila*. Science 2000;288:1825–1828. [PubMed: 10846164]
10. Boutros M, et al. *Genome*-wide RNAi analysis of growth and viability in *Drosophila* cells. Science 2004;303:832–835. [PubMed: 14764878]
11. Ossipova O, Dhawan S, Sokol S, Green JB. Distinct PAR-1 proteins function in different branches of Wnt signaling during vertebrate development. Dev. Cell 2005;8:829–841. [PubMed: 15935773]
12. Putney LK, Denker SP, Barber DL. The changing face of the Na+/H+ exchanger, NHE1: structure, regulation, and cellular actions. Annu. Rev. Pharmacol. Toxicol 2002;42:527–552. [PubMed: 11807182]
13. Donowitz M, Li X. Regulatory binding partners and complexes of NHE3. Physiol. Rev 2007;87:825–872. [PubMed: 17615390]
14. Ro HA, Carson JH. pH microdomains in oligodendrocytes. J. Biol. Chem 2004;279:37115–37123. [PubMed: 15192115]
15. Frantz C, Karydis A, Nalbant P, Hahn KM, Barber DL. Positive feedback between Cdc42 activity and H+ efflux by the Na-H exchanger NHE1 for polarity of migrating cells. J. Cell Biol 2007;179:403–410. [PubMed: 17984318]
16. Wang D, King SM, Quill TA, Doolittle LK, Garbers DL. A new sperm-specific Na+/H+ exchanger required for sperm motility and fertility. Nature Cell Biol 2003;5:1117–1122. [PubMed: 14634667]
17. Yeung T, et al. Membrane phosphatidylserine regulates surface charge and protein localization. Science 2008;319:210–213. [PubMed: 18187657]
18. Giannakou ME, Dow JA. Characterization of the *Drosophila* melanogaster alkalimetal/proton exchanger (NHE) gene family. J. Exp. Biol 2001;204:3703–3716. [PubMed: 11719534]
19. Mustonen P, Lehtonen J, Koiv A, Kinnunen PK. Effects of sphingosine on peripheral membrane interactions: comparison of adriamycin, cytochrome *c*, and phospholipase A2. Biochemistry 1993;32:5373–5380. [PubMed: 8388718]
20. Kooijman EE, et al. An electrostatic/hydrogen bond switch as the basis for the specific interaction of phosphatidic acid with proteins. J. Biol. Chem 2007;282:11356–11364. [PubMed: 17277311]
21. Lemmon MA. Membrane recognition by phospholipid-binding domains. Nature Rev. Mol. Cell Biol 2008;9:99–111. [PubMed: 18216767]
22. Penton A, Wodarz A, Nusse R. A mutational analysis of dishevelled in *Drosophila* defines novel domains in the dishevelled protein as well as novel suppressing alleles of axin. Genetics 2002;161:747–762. [PubMed: 12072470]
23. Zeng X, et al. Initiation of Wnt signaling: control of Wnt coreceptor Lrp6 phosphorylation/activation via frizzled, dishevelled and axin functions. Development 2008;135:367–375. [PubMed: 18077588]
24. Jenny A, Darken RS, Wilson PA, Mlodzik M. Prickle and Strabismus form a functional complex to generate a correct axis during planar cell polarity signaling. EMBO J 2003;22:4409–4420. [PubMed: 12941693]
25. Bizzarri R, et al. Development of a novel GFP-based ratiometric excitation and emission pH indicator for intracellular studies. Biophys. J 2006;90:3300–3314. [PubMed: 16603505]
26. Schwarz-Romond T, Merrifield C, Nichols BJ, Bienz M. The Wnt signalling effector Dishevelled forms dynamic protein assemblies rather than stable associations with cytoplasmic vesicles. J. Cell Sci 2005;118:5269–5277. [PubMed: 16263762]
27. Lang K, Wagner C, Haddad G, Burnekova O, Geibel J. Intracellular pH activates membrane-bound Na(+)/H(+) exchanger and vacuolar H(+)-ATPase in human embryonic kidney (HEK) cells. Cell. Physiol. Biochem 2003;13:257–262. [PubMed: 14586169]

28. Sandvig K, Olsnes S, Petersen OW, van Deurs B. Acidification of the cytosol inhibits endocytosis from coated pits. J. Cell Biol 1987;105:679–689. [PubMed: 2887575]

29. Fang Y, Vilella-Bach M, Bachmann R, Flanigan A, Chen J. Phosphatidic acid-mediated mitogenic activation of mTOR signaling. Science 2001;294:1942–1945. [PubMed: 11729323]

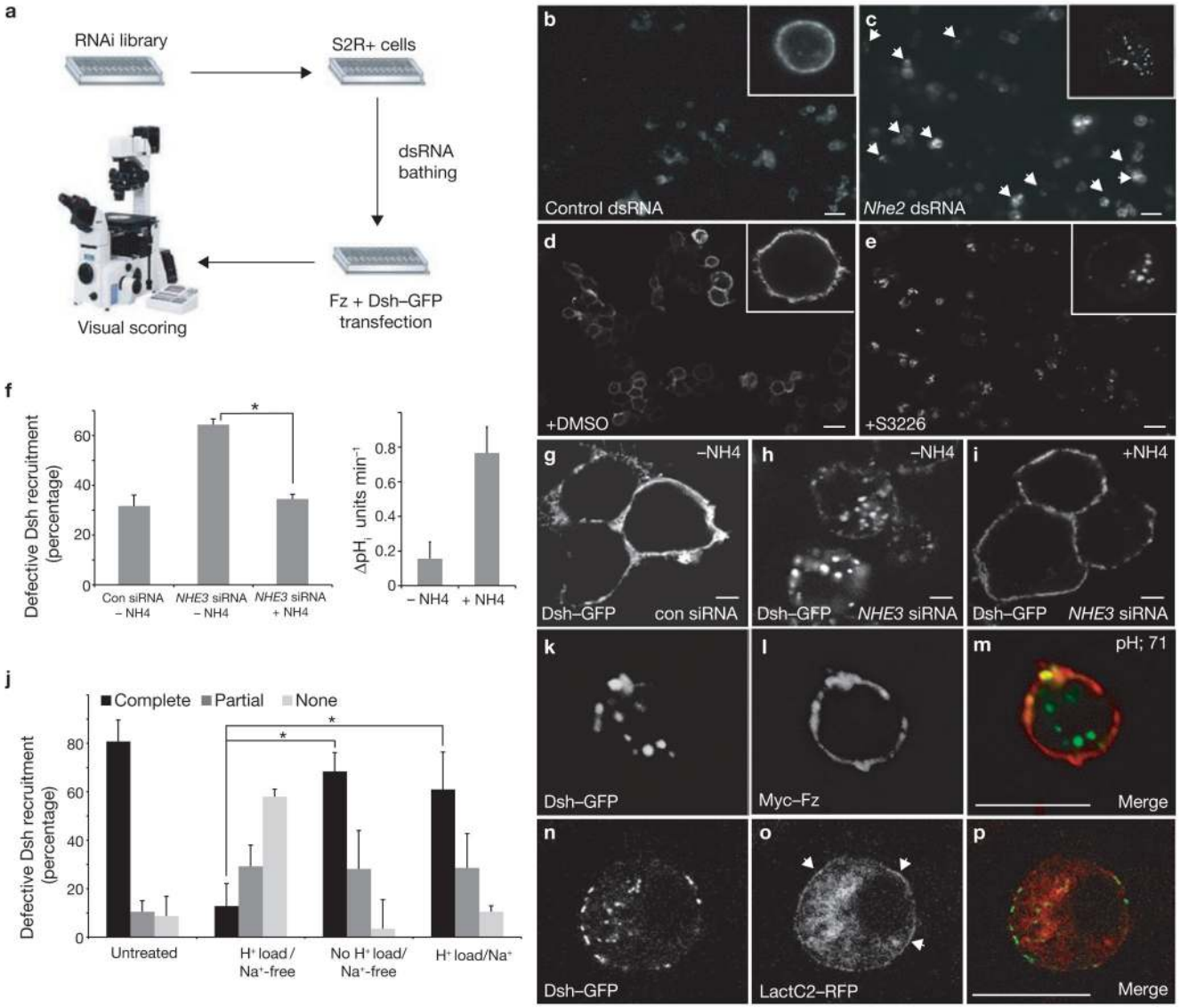

Figure 1.

Nhe2/NHE3 activity is required for Fz-mediated Dsh recruitment. (**a**) Genome-wide RNAi library screen for Fz-mediated Dsh recruitment in *D. melanogaster* S2R+ cells. The cells were plated in 57 384-well plates containing dsRNA against 90% of *D. melanogaster* genes, transfected with *myc–fz* and *dsh–GFP* plasmids and analysed visually (see Methods). (**b**, **c**) Screen hits were defined by a × 20 microscope field with >10 cells showing defective Dsh–GFP recruitment. Control (Relish dsRNA) showed complete recruitment (**b**, see enlarged cell, inset), *Nhe2* dsRNA caused defects in recruitment (**c**), see arrowheads and inset for defects. (**d**, **e**) HEK293T cells expressing Myc–Fz and Dsh–GFP were treated with the NHE3 inhibitor S3226 at 50 μM for 12 h. Treatment led to a redistribution of Dsh–GFP (**e**) as opposed to the control (DMSO) (**d**). (**f**) *NHE3* knockdown caused defective Dsh recruitment (64.3% ± 2.3%, compared with 31.6% ± 4.3% in controls, this baseline defect in Dsh recruitment is due to heterogenous Fz and Dsh expression in these cells). Treatment with 30 mM NH_4Cl to increase pH_i (mean ± s.e.m. from three independent experiments, measured in **f**, right graph) rescued the recruitment defect in *NHE3*-knockdown cells (mean ± s.d., *n*= three independent experiments, **P* < 0.001, measured in **f** left graph). (**g–i**) Alkalinization was transient with

gradual pH normalization within 20 min. Images for all three conditions in **f** are shown. (**j–p**) Intracellular acidification interferes with Dsh recruitment. S2R+ cells were prepulsed for 30 min with 30 mM NH_4Cl and then switched to a Na^+-free medium for 12–16 h. This treatment caused a stable reduction of pH_i to 7.1 (measured by E^2GFP expression[25] and pH calibration), resulting in defective Dsh recruitment (**k–m**). Incubation in a Na^+-free medium without prepulsing (pH_i 7.28) or in Na^+-containing medium after prepulsing (mean ± s.d., n = 4 independent experiments, $*P < 0.001$) mildly affected recruitment. For quantification (**j**), only cells expressing Fz at their cell surface were counted. Note robust recruitment in untreated cells with pH_i 7.45. (**n–p**) In a second assay, pH_i was lowered by applying K^+/nigericin for 4 h and clamping pH_i according to an extracellular buffer (pH 6.8). This did not affect membrane association of the phosphatidylserine-binding LactC2–RFP but did affect Dsh membrane localization. Scale bars represent 10 μm.

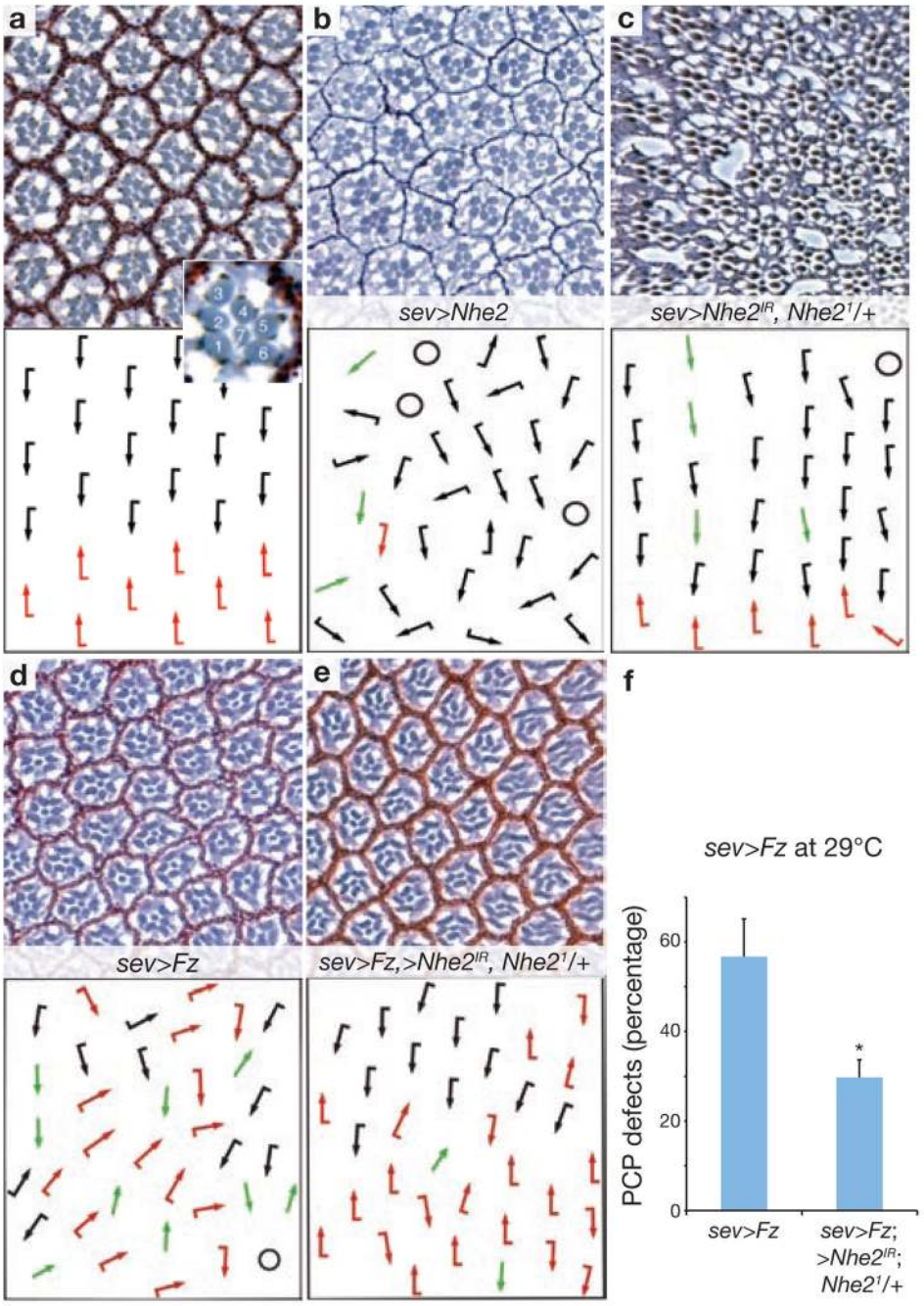

Figure 2.

Nhe2 shows gain- and loss-of-function PCP phenotypes in *D. melanogaster* eye, and interacts genetically with Fz. (**a–e**) show tangential eye sections of adult eyes (upper panels) with respective schematic representations (lower panels). Sections are around the equator (except in **b**, which shows a dorsal area). Wild-type eye with ommatidia of opposing chirality arranged around the equator and R3 positioned at the tip of the trapezoid is shown in **a**. Dorsal and ventral ommatidia are depicted with black and red arrows, respectively. Inset shows enlarged ommatidium with numbered photoreceptor cells. Overexpression of the UAS-*Nhe2*short splice variant (and also the long form, data not shown) with sev>GAL4 caused PCP defects (**b**) consisting of symmetrical clusters (green arrows), rotation defects and occasional chirality

inversions. Extra photoreceptors, as well as fused ommatidia, were also seen. Circles represent unscorable clusters. Knockdown of *Nhe2* and removal of one copy of *Nhe2* (sev>Nhe2^{IR}; Nhe2^{1}/+) led to PCP defects (**c**, 7.11%±3.5%, data are mean ± s.d of three independent eyes with > 400 ommatidia scored). In addition, general defects of eye morphology and structure are commonly seen with this genotype. (**d–f**) The sev>Fz phenotype is suppressed by co-expression of UAS-Nhe2^{IR} and removal of one *Nhe2* copy. This experiment was performed at 29 °C to enhance Fz and Nhe2^{IR} expression. Total PCP defects were scored and quantified (**f** , data are mean ± s.d. of six eyes with > 700 ommatidia scored, **P* < 0.0001).

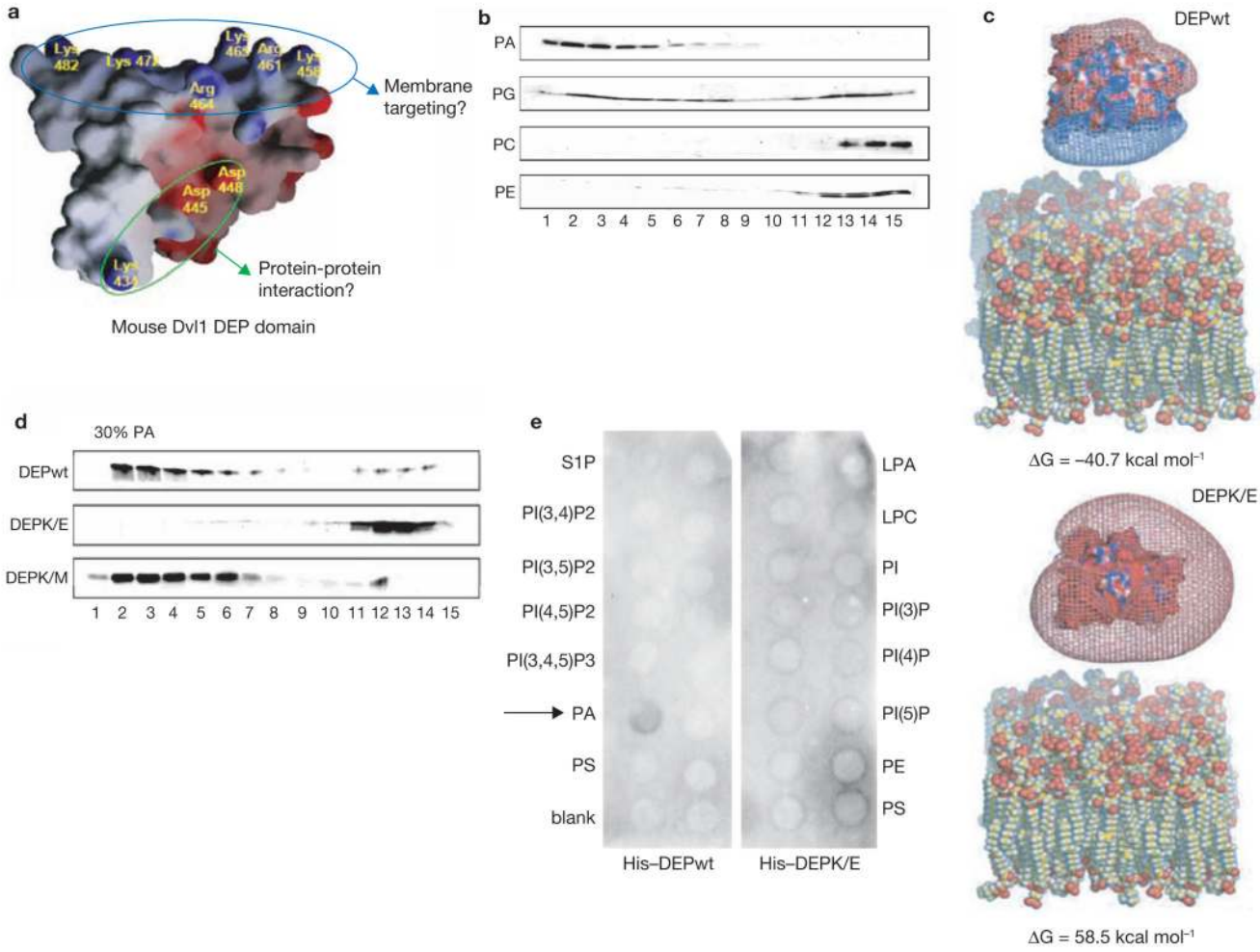

Figure 3.

The Dsh DEP domain interacts with acidic phospholipids. (**a**) The solution structure of the DEP domain of mouse Dvl1 shows a polybasic amino acid stretch positioned at a different surface location than the electric dipole for putative protein–protein interaction (which includes the lysine mutated in *dsh*^{1}-K/M)[8]. (**b**) SUV liposomes consisting of 50% PC and 50% of the indicated phospholipids were mixed with the Dvl1 DEP domain and separated by chromatography on a Sephacryl S-300 column. The column fractions were analyzed by silver-staining. The lipid-bound DEP domain was eluted from fractions 1 to 7, whereas free DEP domain was eluted from fractions 10 to 15. (**c**) Electrostatic potentials were calculated using the non-linear Poisson-Boltzmann equation, to model phospholipid bilayers containing a 1:1 mixture of PC and PA. The complexity of the structures of DEPwt, DEPK/E and the lipid membrane model was minimized using a molecular dynamic simulation method (see Methods). The binding energy (ΔG) between DEPwt and the acidic lipid membrane model was predicted to be −40.7 kcal mol^{-1} (upper panel). However, for the DEPK/E mutant an unfavorable binding energy of 58.5 kcal mol^{-1} was calculated (lower panel). (**d**) SUV liposomes containing 70% PC and 30% PA were mixed with DEPwt, DEPK/E and DEPK/M (Lys 434, see **a** for location of mutations); binding to DEPK/E was markedly decreased. The overall structure of the isolated Dvl1 DEP domain was not affected by the K/E mutations as determined by chemical shift patterns from NMR spectroscopy (data not shown). Full scans of **b** and **d** are shown in Supplementary Information, Fig. S6. (**e**) Nitrocellulose filters (PIP strips) spotted with several

different phospholipids species were overlayed with His-tagged DEPwt and DEPK/E (1 μg ml^{-1}) and subjected to western blotting with a monoclonal anti-His antibody. DEPwt bound specifically to PA (arrow). DEPK/E did not bind to any of the spotted phospholipids. LPA, lysophosphatidic acid; LPC, lysophosphatidylcholine; PI, phosphatidylinositol; $PIXP_n$, phosphatidylinositol X $phosphate_n$; PE, phosphatidylethanolamine; PC, phosphatidylcholine; S1P, sphingosine-1-phosphate; PA, phosphatidic acid; PS, phosphatidylserine.

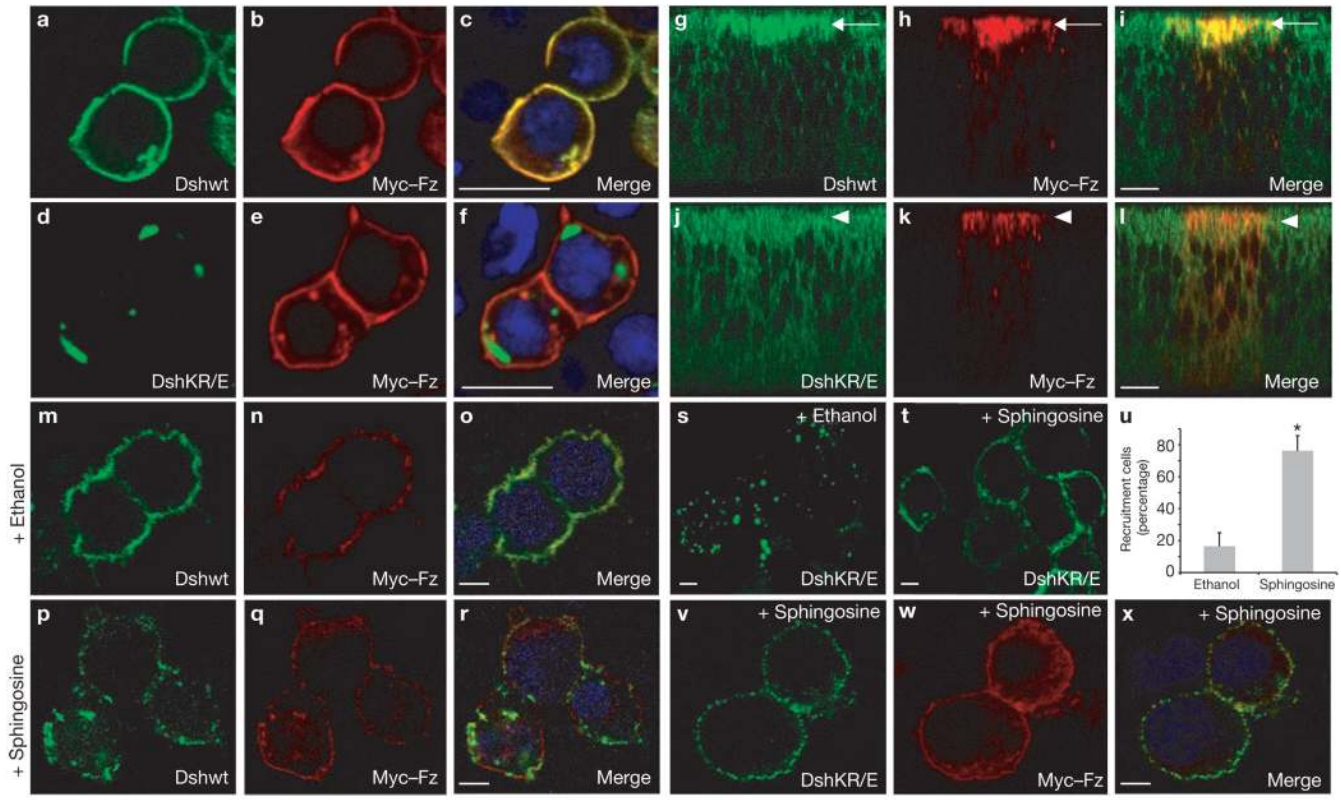

Figure 4.

Fz-mediated Dsh membrane recruitment is charge-dependent. (**a–f**) DshKR/E(5×)–GFP, bearing five lysine or arginine substitutions for glutamic acid, was no longer recruited by Fz in S2R+ cells (**d–f**). The mutated amino acids correspond to the conserved residues mutated in mouse Dvl1 DEP-K/E. Fz efficiently recruited Dshwt (**a**–**c**). Fz was visualized with a monoclonal anti-Myc antibody. Dsh-(KR/E) is expressed in higher amounts than Dshwt, as shown by western blotting (Supplementary Information, Fig. S5b). Merged panels (**c**, **f**) also include Hoechst 33342 (blue) as nuclear stain. (**g–l**) DshKR/E–GFP shows defective recruitment to the apical junctions by Myc–Fz in third-instar wing discs *in vivo*. Dshwt–GFP (**g**) and DshKR/E–GFP (**j**) were expressed ubiquitously under endogenous *dsh* promoter sequences. Myc–Fz (**h, k**) was expressed in a stripe at the anterior-posterior boundary using *dpp>GAL4*. Displayed is a *x*/*z*-stack of wing epithelial cells with apical at the top and basal at the bottom. Unlike Dshwt–GFP (arrows, **g–i**), DshKR/E–GFP is not recruited to the apical membrane by Fz (arrowheads, **j–l**). Other than the dpp stripe, the expression strength and localization patterns of Dshwt and DshKR/E(5×) are indistinguishable (**g, j**). (**m–r**) Neutralization of negatively charged membrane lipids (such as PA) by the membrane-permeant weak base sphingosine (75 μM), affects Dsh–GFP localization in HEK293T cells. The overlap of Dsh and Fz at the plasma membrane is diminished (**p–r**), compared with control vehicle-treated (**e**thanol) cells (**m–o**). Partial internalization of both proteins is also seen. The same pattern is observed in S2R+ cells, data not shown. (**s–u**) Sphingosine rescues the defective recruitment of DshKR/E–GFP by Fz. Sphingosine (75 μM) and ethanol were applied for 3 h. Sphingosine rescue was quantified (**u**), data are mean ± s.d, n = 10 different microscope fields from two experiments, **P* < 0.0001. (**v–x**) DshKR/E–GFP co-localizes with Fz in sphingosine-rescued cells.

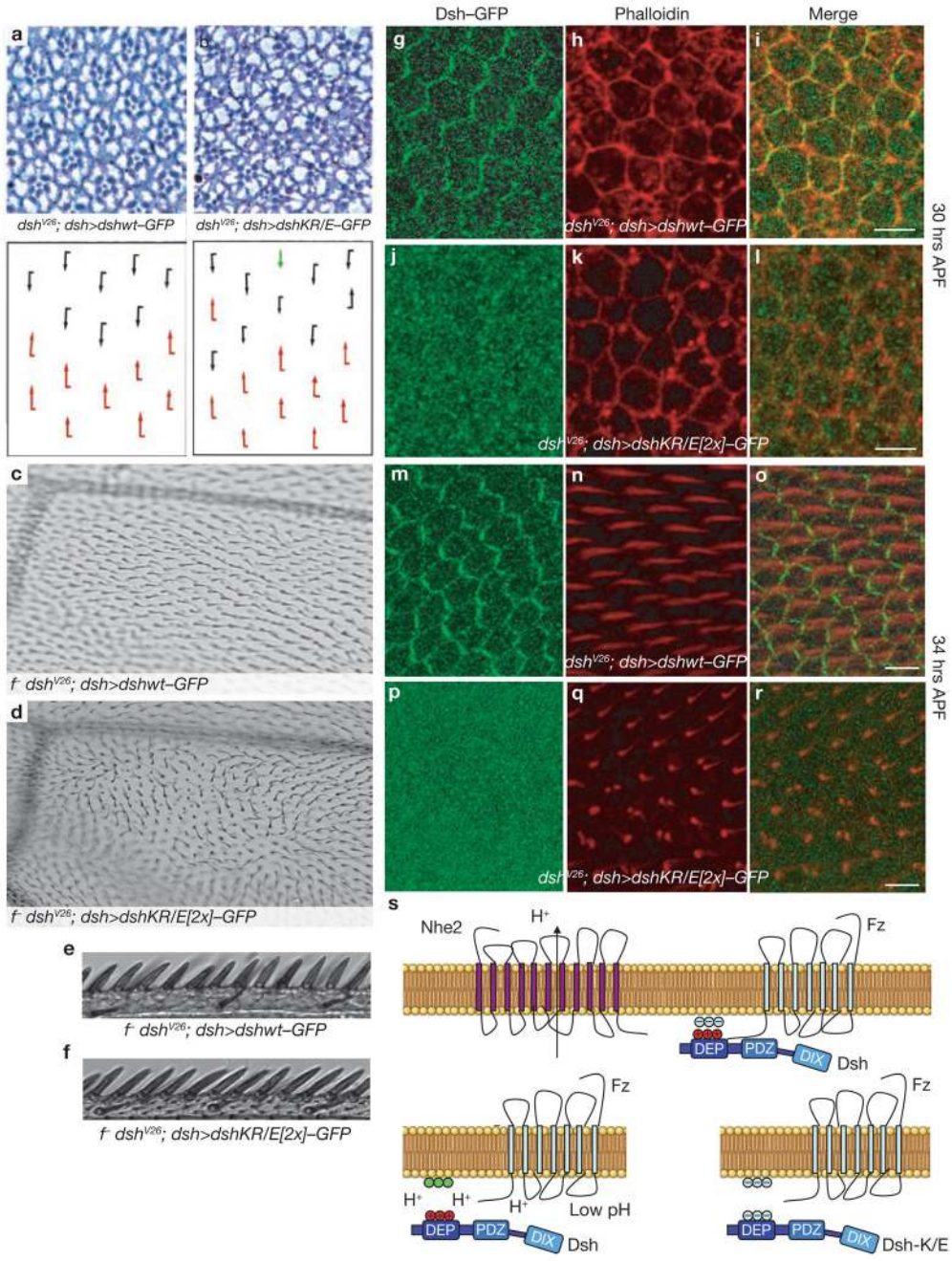

Figure 5.

The polybasic stretch in the Dsh DEP domain is essential for PCP signalling *in vivo*. Dshwt–GFP and DshKR/E–GFP were expressed under a *dsh* promoter in a dsh^{V26} null background (dsh^{V26}*; dsh>dsh–GFP*). (**a–r**) Flies that rescued the dsh^{V26} lethality were scored for phenotypes in adult eyes (**a, b**, schematic representations lower panels, dorsal and ventral ommatidia are depicted with black and red arrows respectively, the green arrow depicts a symmetrical cluster), adult wings (**c–f**) and pupal wings (**g–r**). In the eye, DshKR/E(2×) caused mild phenotypes, including symmetrical clusters, chirality inversions and rotation defects (**b**). In adult wings, DshKR/E(2×) caused severe defects in wing-hair orientation, whereas the complete wing margin was intact (**d**). The anterior wing margin bristles are shown for DshKR/

E(2×) (**f**), and Dshwt (**e**). Rescue with Dshwt was complete with fully wild-type appearance (**a, c, e**). (**g–r**) Pupal wings were examined at a stage before wing-hair formation (~30 h APF, **g–l**) and during wing hair formation (~34 hours APF, **m–r**). Dshwt–GFP co-localized with phalloidin-stained actin at the cell cortex at the early stage (**g–i**). In contrast, DshKR/E(2×)–GFP showed diffuse cytoplasmic localization (**j–l**). At the later stage (~34 h APF), Dshwt–GFP showed a typical cortical distribution with enrichment in the proximo-distal axis, and wing hairs showed a normal proximo-distal orientation (**m–o**, as reflected by Phalloidin, red). DshKR/E(2×)–GFP also failed at this stage to associate with the membrane (**p–r**). The resulting phenotypes are misoriented wing hairs and a multiple wing hair phenotype (**q–r**). Wing hairs appear shorter than shown in **n**, as the misoriented hairs point up and out of the confocal plane. (**s**) Suggested model of Fz-mediated Dsh membrane recruitment. Dsh binds weakly via its PDZ domain to the Fz C terminus. In addition, the DEP domain binds directly to acidic phospholipids. The interaction is dependent on local pH and charge. With Dshwt , proximity of the Na^+/H^+ exchanger Nhe2 to Fz maintains a slightly basic local pH (upper panel). When local pH is lower (*Nhe2* mutant), the lipid headgroups are protonated, losing their negative charge (green) and leading to repulsion of Dsh (lower left panel). Similarly, mutations in the polybasic stretch of the DEP domain cause cytoplasmic Dsh localization (lower right panel), which can be rescued by lowering surface negativity (Fig. 4s–u). It is possible that another surface of the DEP domain also interacts with Fz directly.